Available online at www.sciencedirect.com
ScienceDirect
Bioelectrochemistry 69 (2006) 117–125
Bioelectrochemistry
www.elsevier.com/locate/bioelechem

Microfluidic electroporation of robust 10-μm vesicles for manipulation of picoliter volumes

Eunice S. Lee, David Robinson, Judith L. Rognlien, Cindy K. Harnett, Blake A. Simmons, C.R. Bowe Ellis, Rafael V. Davalos *

Sandia National Laboratories, P.O. Box 969, Livermore, CA 94551, USA

Received 2 August 2005; received in revised form 1 December 2005; accepted 12 December 2005
Available online 17 February 2006

Abstract

We present a new way to transport and handle picoliter volumes of analytes in a microfluidic context through electrically monitored electroporation of 10–25 μm vesicles. In this method, giant vesicles are used to isolate analytes in a microfluidic environment. Once encapsulated inside a vesicle, contents will not diffuse and become diluted when exposed to pressure-driven flow. Two vesicle compositions have been developed that are robust enough to withstand electrical and mechanical manipulation in a microfluidic context. These vesicles can be guided and trapped, with controllable transfer of material into or out of their confined environment. Through electroporation, vesicles can serve as containers that can be opened when mixing and diffusion are desired, and closed during transport and analysis. Both vesicle compositions contain lecithin, an ethoxylated phospholipid, and a polyelectrolyte. Their performance is compared using a prototype microfluidic device and a simple circuit model. It was observed that the energy density threshold required to induce breakdown was statistically equivalent between compositions, 10.2 ± 5.0 mJ/m^2 for the first composition and 10.5 ± 1.8 mJ/m^2 for the second. This work demonstrates the feasibility of using giant, robust vesicles with microfluidic electroporation technology to manipulate picoliter volumes on-chip.

Keywords: Electroporation; Electropermeabilization; Giant vesicle; Giant liposome; Sample management

1. Introduction

In microfluidics, diffusion and nonuniform flow velocities (particularly from pressure-driven flow) often cause unwanted mixing and dilution, resulting in broad, nonuniform concentration profiles and reaction rates. These effects can seriously degrade device performance when only trace amounts of sample material are available. A design strategy to overcome these challenges is to keep analytes in confined volumes to improve mass transport in the microfluidic device. Immiscible fluids [1] and bubbles [2] have been employed by researchers to isolate analytes and circumvent these obstacles. Each of these methods has its inherent advantages and disadvantages. In this method, giant vesicles (10–25 μm) are used to isolate analytes in a microfluidic environment. Once encapsulated inside a vesicle, contents will not diffuse and become diluted when exposed to pressure-driven flow. To the best of our knowledge, this study presents the first demonstration of giant vesicle electroporation in a microfluidic environment. This study offers a new, practical and simple strategy to handle picoliter volumes in a microfluidic device through autonomous electrical control of biomimetic cell-sized containers.

Rapid electric pulses can be used to enhance the permeability of a cell membrane for the introduction of impermeable molecules into a biological cell through a phenomenon known as electroporation [3,4]. During electroporation, the electric field charges the membrane, changing the electrochemical potential across it [3,4]. As a function of this potential difference as well as other external factors, the pulses can have no effect on the membrane, reversibly open the membrane, or irreversibly open the membrane. Progress has been made toward the application of this technique on individual cells using ultra-microelectrodes [5] and microfluidic platforms for improved control of the reversible permeation of the cell membrane [6–9].

* Corresponding author. Tel.: +1 925 294 3504; fax: +1 925 294 3866.
E-mail address: rvdaval@sandia.gov (R.V. Davalos).

1567-5394/$ - see front matter © 2005 Elsevier B.V. All rights reserved.
doi:10.1016/j.bioelechem.2005.12.002

Giant vesicles (10–25 μm diameter) are of recent interest to explore the rapid chemical kinetics of molecules within a confined nanoenvironment because of their relatively large size and their artificial phospholipid membrane, which closely resembles the membranes of living cells [10–12]. Researchers have demonstrated the utility of giant lipid vesicles through off-chip manipulation techniques such as micro-injection with borosilicate microneedles [10–12] and optical trapping with focused laser beams [13]. Analytes can be loaded into or out of vesicles by electroporation as well, as demonstrated with patch clamp systems [10–12] and with micromanipulator-controlled ultramicroelectrodes [10–12] in non-microfluidic environments.

Various preparation methods of giant vesicles have been reported, including electroformation [14–17], the evaporation of a nonaqueous lipid solution, film hydration, and dispersal in an aqueous buffer [18,19]. We have found previous preparations unsuitable for our microfluidic applications due to problems with reproducibility and vesicle strength under electrical and/or mechanical stress. In this paper, we describe two improved preparation schemes of giant vesicles that we have developed that can withstand electrical and mechanical manipulation in microfluidic devices, and we compare their performance as they are integrated into a prototype platform. These two methods produced a larger fraction of vesicles containing analytes, such as dye, compared to previous published methods [18,19].

The combination of giant robust vesicles with electrically-monitored electroporation is the first step towards a microfluidic platform in which samples are autonomously moved and manipulated through a number of sample loading stations, guided only by electrical feedback. These manipulations include loading analyte into the vesicle, transporting the vesicle between loading stations, releasing analyte from the vesicle, and even fusing of vesicles to combine encapsulated analytes [20] all while overcoming many of the unwanted effects associated with microfluidics. While many of these tasks remain to be demonstrated in order to integrate all of these functions and overcome the limits of pressure-driven flow, we have shown that several of the key steps are achievable.

2. Experimental and analytical methods

2.1. Materials

Three lipids were used: 1,2-Dioleoyl-*sn*-Glycero-3-Phosphoethanolamine-*N*-[Methoxy(Polyethylene glycol)-2000] (Ammonium Salt) (PEGDOPE), L-α-phosphatidylcholine (Soy—95%) (Lecithin), and 1,2-distearoyl-*sn*-Glycero-3-Phosphoethanolamine (PEGDSPE) (Avanti Polar Lipids, Inc., Alabaster, AL). Alexa Fluor 488 carboxylic acid, succinimidyl ester dye was used to visually verify electroporation (Molecular Probes, Inc., Invitrogen Detection Technologies, Eugene, OR). Other materials were purchased from Aldrich (Sigma-Aldrich Corp., St. Louis, MO). Poly (tetrapropylammonium acrylate) was prepared by adding one equivalent of 0.5 M tetrapropylammonium hydroxide to M_w 16,000 poly(acrylic acid) and removing water under vacuum. 0.4 M poly(Me_4N acrylate) was prepared similarly. $(Pr_4N)_2$ glutarate is prepared by hydrolyzing glutaric anhydride with tetrapropylammonium hydroxide. 75 mM $(Me_4N)_2$ glutarate was made by adding 114 mg of glutaric anhydride to 12.6 mL DI water, then adding 0.72 mL of tetramethylammonium hydroxide, then titrating to pH 7 with the addition of glutaric anhydride.

2.2. First giant vesicle preparation method—PEGDOPE : lecithin

To develop vesicles that are robust enough to withstand a microfluidic environment, preparation methods were developed by modifying Yamashita's method [19]. Initially, a 50 mM lipid stock solution was made by adding 10 mg PEGDOPE and 160 mg lecithin (1 : 50 PEGDOPE : lecithin) to 2 mL filtered chloroform. A stock dye solution was prepared by adding 1 mL DI water to a vial containing 1 mg (subsequently hydrolyzed) succinimidyl Alexa Fluor 488 carboxylate dye. 120 μL of 1 : 50 PEGDOPE : lecithin stock solution was then combined with 1.2 μL of the dye stock solution.

100 mg poly(tetrapropylammonium acrylate) was added to 3.2 mL filtered chloroform to make a stock polyelectrolyte solution.

20 μL PEGDOPE–lecithin–dye solution was pipetted into a 4-mL vial, and 1 μL of polyelectrolyte solution was then added.

The chloroform was evaporated by gently blow drying under a nitrogen stream. The open vial was placed under vacuum overnight at room temperature to completely evaporate the chloroform.

After drying, 2 μL DI water was added as a drop on the sidewall of the vial. The vial was capped and placed in a 37 °C oven for 10 min, forming a hydrated film. A capped vial of filtered 75 mM $(Pr_4N)_2$ glutarate in water was also heated at 37 °C for ten minutes.

The vials were then removed from the oven, and 1 mL of 75 mM $(Pr_4N)_2$ glutarate was pipetted into the vial of lipid–dye–polyelectrolyte solution. The capped vial was incubated at 37 °C for 1 h.

2.3. Second giant vesicle preparation method—PEGDSPE : lecithin

Initially, a 50 mM lipid stock solution was made by adding 10 mg PEGDSPE and 160 mg lecithin (1 : 50 PEGDSPE : lecithin) to 2 mL filtered ethanol. A stock dye solution was prepared by adding 1 mL DI water to a vial containing 1 mg (subsequently hydrolyzed) succinimidyl Alexa Fluor 488 carboxylate dye. 120 μL of 1 : 50 PEGDSPE : lecithin stock solution was then combined with 1.2 μL of the dye stock solution.

20 μL PEGDSPE–lecithin–dye solution was pipetted into a 4-mL vial, and 10 μL polyelectrolyte solution, 0.4 M poly (Me_4N acrylate) in ethanol, was then added to the vial. The ethanol was evaporated by gently blow drying under a nitrogen

stream. The open vial was placed under vacuum overnight at room temperature to completely evaporate the chloroform.

After drying, 2 μL DI water was added as a drop on the sidewall of the vial. The vial was capped and placed in a 37 °C oven for 10 min, forming a hydrated film. A capped vial of filtered 75 mM Me_4N glutarate was also heated at 37 °C for ten minutes.

The vial was then removed from the oven, and 1 mL of 75 mM Me_4N glutarate was pipetted into the vial of lipid–dye–polyelectrolyte solution. The capped vial was incubated at 37 °C for 2 h.

2.4. Microfluidic electroporation technology

We have developed a prototype microfluidic platform utilizing a four-electrode geometry to deliver and sense electric pulses. With this configuration, it is possible to immobilize individual vesicles on low-pressure ports, electrochemically open and close them, and monitor their porosity by measuring electrical current passing through the vesicle walls. The test platform (Fig. 1(A,B)) consists of two fluidic chambers (outfitted with electrodes) that are interconnected through a pore using standard silicon microfabrication technology [7,8,21]. The platform incorporates a replaceable silicon chip with a supported 1 × 1 mm, 1 μm thick dielectric silicon nitride membrane on which a pore (6 μm in diameter) is patterned. The pore edges have abrupt right angles and are typical of edges commonly made in microfluidic designs; edge shape is known to be an important consideration [22].

A platinum electrode (Omega Engineering, Inc.) is placed in each of the fluidic chambers, to apply a voltage signal across the vesicle trapped in the test platform, and a silver/silver chloride (Ag/AgCl) electrode (In Vivo Metric, Healdsburg, CA) is placed in each of the fluidic chambers to sense the potential difference across the pore. The top chamber is open on top and acts as an inlet port for easy sample introduction using a pipette, and the bottom chamber is optically transparent for visual inspection using an inverted microscope. The two chambers are then filled with conductive solutions, and an aliquot of vesicles can then be introduced into the top chamber by simply using a pipette. In this configuration, hydrostatic pressure is applied as suction through a hand-controlled syringe pump to immobilize a single vesicle on the pore. A pressure transducer (Senstronic USA, San Francisco, CA) is also connected to the test platform, allowing the delivery of electroporation signals to the immobilized giant vesicle at a consistent pressure.

2.5. Electrical test and measurement system

The electrical test and measurement system consists of voltage delivery and measurement circuitry, a software-driven system controller (Labview, National Instruments, Austin, TX), a computer-controlled interface card (National Instruments, Austin, TX), and a commercially-purchased pressure transducer (Senstronic USA, San Francisco, CA).

The voltage delivery and measurement circuitry are illustrated in Fig. 2. A dual power supply (±15 V) is used to power the electronics. A voltage ramp waveform, developed in Labview, is delivered to the test platform using the platinum electrodes. The output current is measured using an op-amp (OP07c, Texas Instruments) configured as a current-to-voltage converter. The electric potential difference across the pore is measured using the Ag/AgCl electrodes and an instrumentation op-amp (AMP02E, Analog Devices). Using this four-electrode setup, voltage-controlled feedback is implemented using a drive op-amp (OP07c, Texas Instruments) to minimize electrochemical drift in the measured signals. The output voltage (V_{out}) and current (I_{out}) are recorded using Labview.

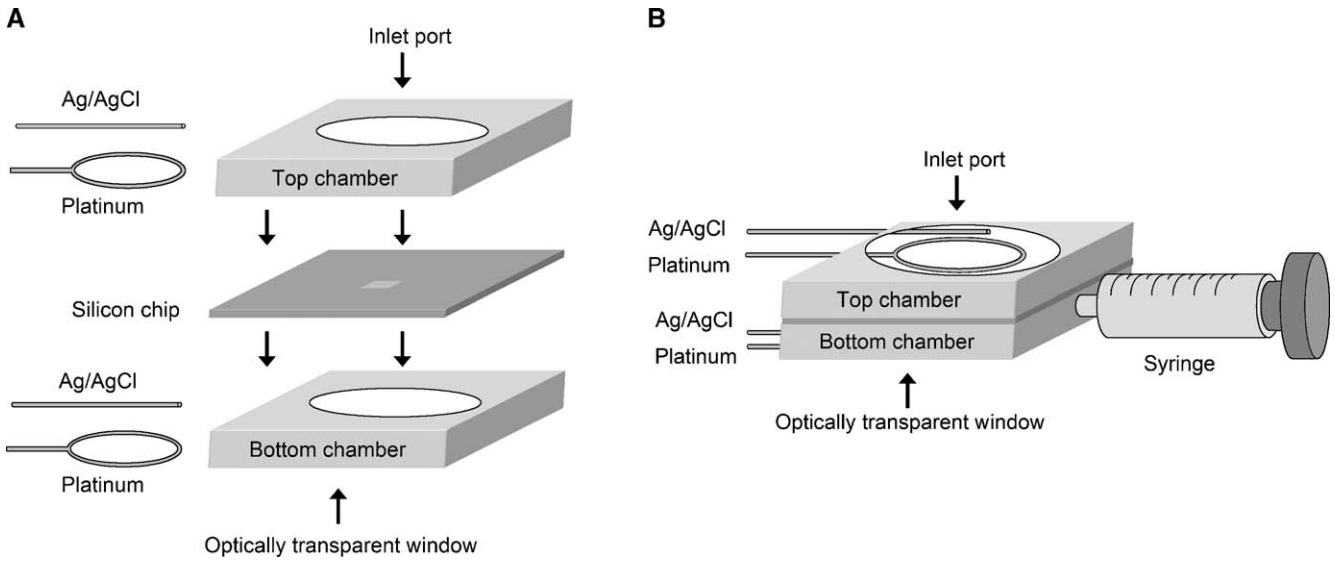

Fig. 1. (A) View of the test platform prior to assembly. The top chamber contains an inlet port for sample introduction and the bottom chamber contains a transparent window for visual inspection using a microscope. (B) Complete view of the assembled test platform. A manual syringe pump is attached to apply negative pressure.

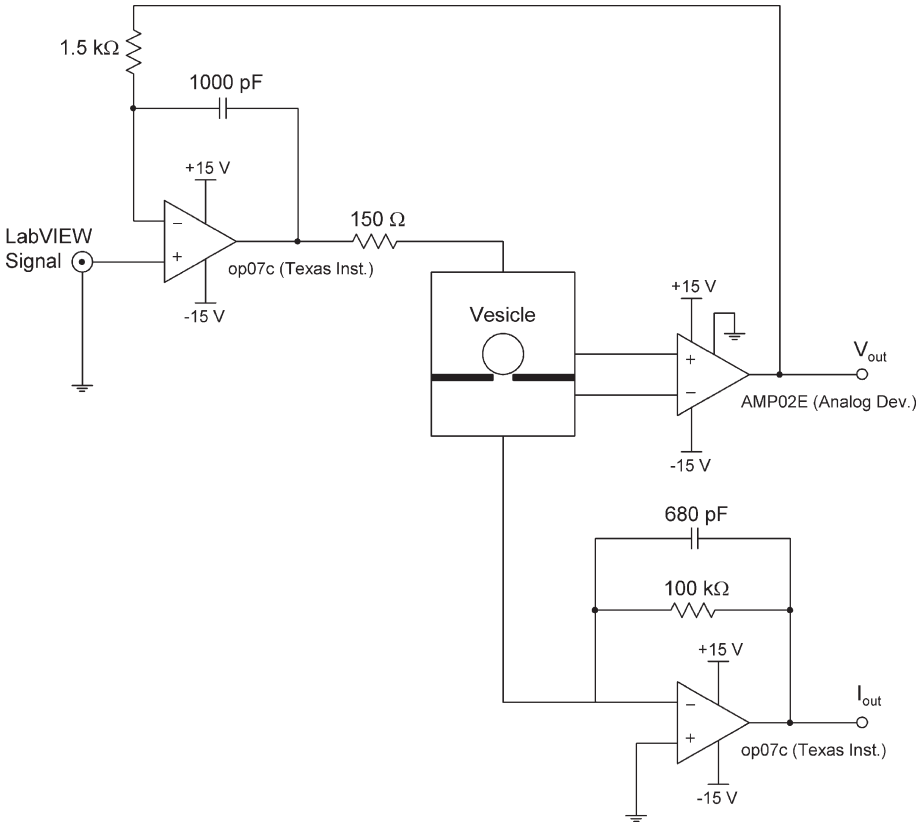

Fig. 2. Voltage delivery and sensing circuitry.

When a giant vesicle is immobilized on the pore, the vesicle is allowed to sit for 30 s. The applied pressure is then measured using a pressure transducer and recorded prior to voltage delivery using Labview.

2.6. Theoretical Model

One method to compare the mechanical and electrical performance of the two vesicle compositions in our microfluidic device is to use the simple and elegant energy-based model of the membrane presented by Evans for aspiration of vesicles with a micropipette [23]. In this model, the energy stored per unit area of the vesicle membrane, T, is the sum of the electrical, T_E, and mechanical, T_M, energy. Breakdown of the membrane, or the onset of electroporation, occurs when this energy density exceeds a critical threshold. This model assumes applied pressure causes a portion of the vesicle to deform into a hemisphere near the pore while the rest of the vesicle remains spherical (Fig. 3). In addition, no chemical adhesion of the vesicle to the surface of the pore occurs in this model. The different components of the energy associated with the vesicle membrane can be expressed as:

$$T = T_M + T_E \tag{1}$$

$$T_M = \frac{\Delta P r_p/2}{1-r_p/r_v} \tag{2}$$

where ΔP is the applied pressure across the vesicle membrane, r_p is the radius of the pore, and r_v is the radius of the giant vesicle.

$$T_E = \frac{1}{2} C_s V_T^2 = \frac{1}{2}\frac{\varepsilon\varepsilon_0}{t} V_T^2 \tag{3}$$

where C_s is the capacitance of the membrane per unit area, V_T is the transmembrane potential, ε_0 is the permittivity of free space (8.85×10^{-12} F/m), ε is the relative permittivity of the vesicle membrane and t is the thickness of the vesicle membrane. In this study, we assumed the values $\varepsilon=2.2$ and $t=4\times10^{-9}$ m, as previously used by Needham [12].

To determine V_T, a circuit model, shown in Fig. 3(B), is used to represent our microfluidic device containing an immobilized vesicle. The four-electrode system allows us to neglect the resistive and capacitive effects of the source electrodes. In this analysis the potential drops due to the resistance of the bulk solution and the internal vesicle solution resistance are assumed to be negligible, so only the potential drop across the membranes is considered. The immobilized vesicle itself is modeled such that the circuit path enters the vesicle through one side of the membrane (modeled as a parallel combination of a resistive R_{MEM1} and capacitive C_{MEM1} component), passes through the intracellular space of the vesicle (represented by a resistive R_I element), and exits the vesicle through the other side of the membrane (modeled as another parallel combination of a resistive R_{MEM2} and capacitive C_{MEM2} component). In parallel with the vesicle is a leak resistance, R_{LEAK}. When the vesicle is

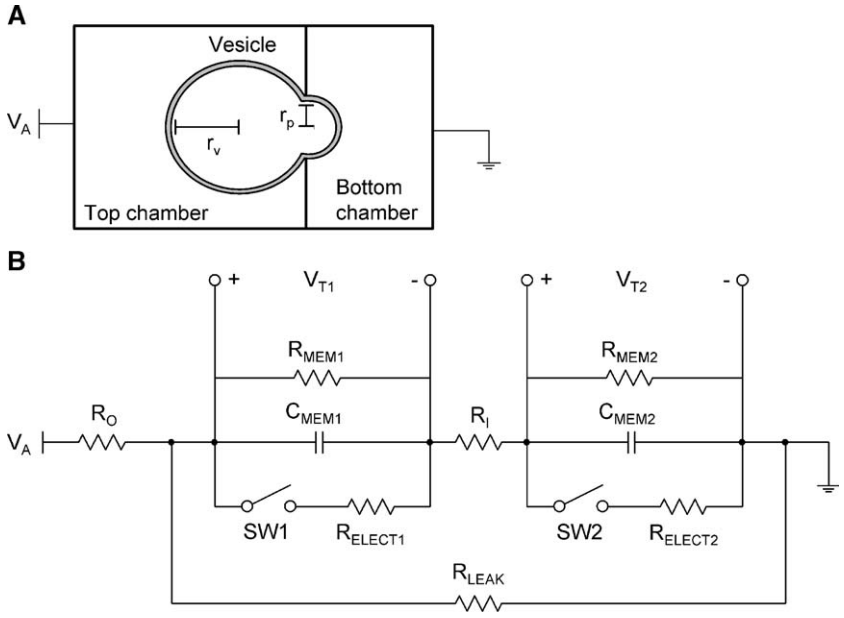

Fig. 3. (A) Schematic of vesicle trapped on pore. (B) Circuit model of microfluidic device containing an immobilized vesicle on the pore.

exposed to an external voltage, V_A, such that the energy density exceeds a critical threshold, electroporation takes place. At this point, the switches, SW1 and SW2, close, causing the total resistance of the membrane to decrease due to the parallel addition of the variable resistors, R_{ELECT1} and R_{ELECT2}. Subsequently, an increase in current can be seen. The transmembrane potential across each of the two membrane areas is represented by V_{T1} and V_{T2}, which their summation can then be approximated by V_A, the applied potential.

$$V_A \approx V_{T1} + V_{T2} \tag{4}$$

Since the surface area of the membrane mated with the pore is much smaller than the surface area of the remaining vesicle and the value of a capacitor is directly proportional to the surface area, the value of C_{MEM2} is much smaller than the value of C_{MEM1}. Therefore, the majority of the potential drop will be across the membrane mated with the pore. For this reason, we are interested in calculating the transmembrane potential of the vesicle membrane mated with the pore, V_{T2}. Following Ohm's Law ($V=IR$), the current through both membranes must be equal.

$$\frac{V_{T1}}{R_{MEM1}} = \frac{V_{T2}}{R_{MEM2}} \tag{5}$$

where R_{MEM1} and R_{MEM2} can be calculated using the membrane resistivity ρ, the membrane thickness t, and the surface areas, A_1 and A_2, of the membranes being permeated. The surface area, A_2, of the membrane mated with the pore is approximated using $A_2 \approx 2\pi r_p^2$. The surface area, A_1, of the remaining membrane is found using $A_1 \approx 4\pi r_v^2 - A_2$. Therefore,

$$\frac{V_{T1}}{\rho t/A_1} = \frac{V_{T2}}{\rho t/A_2} \tag{6}$$

$$V_{T1} = V_{T2}\frac{A_2}{A_1} \tag{7}$$

Finally, V_{T2}, can be calculated using Eqs. (4) and (7):

$$V_{T2} \approx \frac{V_A}{1+\frac{A_2}{A_1}} \tag{8}$$

From Eqs. ((1)–(8)), we can obtain a value for the total stress, T, on the vesicle as a function of the applied voltage, pressure and vesicle radius.

$$T = \frac{1}{2}\frac{\varepsilon\varepsilon_0}{t}\left(\frac{V_A}{1+\frac{r_p^2}{2r_v^2-r_p^2}}\right)^2 + \frac{\Delta P r_p/2}{(1-r_p/r_v)} \tag{9}$$

This model allows us to quantitatively compare the mechanical and electrical properties of different size vesicles. This model holds when r_p is less than r_v. This equation is used rather than Schwan's transmembrane potential equation [24] because the vesicle is immobilized onto a pore rather than suspended in solution. Therefore, the model must account for pressure applied to the vesicle and the difference in field distribution due to a boundary (the silicon chip).

3. Results and discussion

3.1. Giant vesicle preparation

Giant vesicles for microfluidic applications need to be robust enough to withstand the electrical and mechanical stresses associated with such environments. Specifically, for lab-on-a-chip, single-cell electroporation, the vesicle must be able to withstand the stresses associated with being pneumatically trapped, repeatedly electroporated, and loaded with compounds of interest. To this end, we have developed an improved preparation scheme by modifying Yamashita's previous method [19]. Although vesicles prepared using this

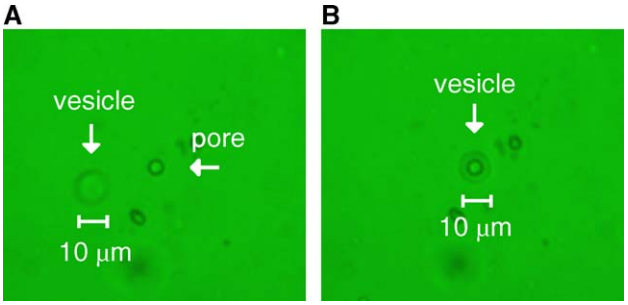

Fig. 4. (A) Optical image of a giant vesicle (10 μm diameter) approaching the pore. (B) Optical image of the giant vesicle immobilized on the pore.

previous method are able to contain a modest salt concentration due to the attachment of poly(ethylene glycol) to the membrane, these vesicles tend to shrivel in shape. We found that including a polyelectrolyte (poly tetrapropylammonium acrylate) in the first vesicle composition appears to favorably bias the osmotic pressure in the vesicle, keeping sufficient tension on the vesicle membrane while it is subject to both pressure gradients (for trapping) and electric fields (for electroporation). By changing the difference in refractive index with respect to the external buffer, the polymer may also improve contrast in an optical microscope. The polymer also serves as a buffer inside the vesicle, in addition to the glutarate both inside and outside the vesicle, keeping the pH at about 7.

Analytes can be loaded into the vesicle either during the hydration step [19] or more efficiently by including it in the lipid film, as long as it is stable in the solvent used for the lipid. This was investigated using Alexa Fluor 488 dye. In the first vesicle composition, although the dye in the dry lipid film resulted in strong fluorescence intensity, some but not all vesicles contained dye, suggesting that the dye was not well dispersed or that some vesicles sealed more quickly than others (an observed correlation between vesicle size and fluorescence intensity supports the latter). In the second preparation method, we found that using this hydrophilic dye in an ethanol-based lipid solution, rather than a chloroform-based lipid solution, substantially improved the mixing of the two materials, greatly enhancing the reproducibility of large-scale preparations of giant vesicles containing analytes, such as dye.

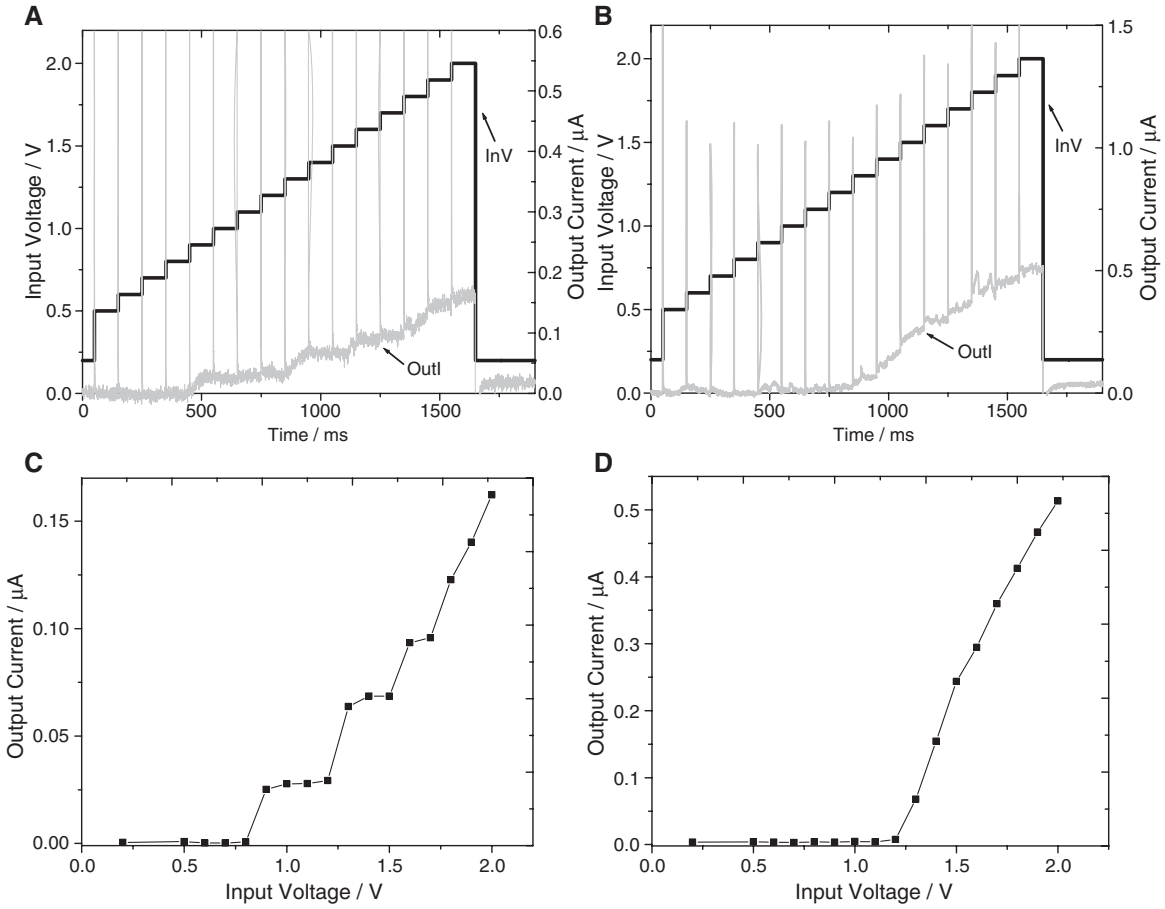

Fig. 5. (A) Typical input voltage (InV) and output current (OutI) as a function of time for a giant vesicle prepared using the first scheme and (B) typical input voltage (InV) and output current (OutI) as a function of time for a giant vesicle prepared using the second scheme. (C) Output current versus input voltage for the same giant vesicle prepared using the first method, and (D) output current versus input voltage for the same giant vesicle prepared using the second method. In all cases, a constant R_{LEAK} was subtracted out from the output current.

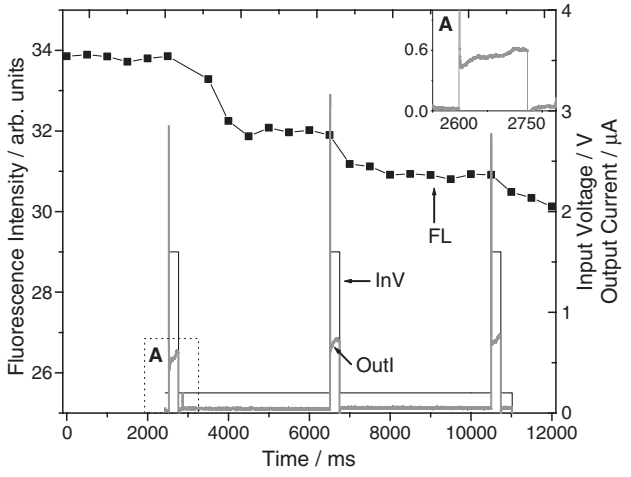

Fig. 6. Typical input voltage (InV), output current (OutI) and fluorescence intensity (FL) for a single trapped giant vesicle as a function of time. Magnified inset (top right corner) shows increase in output current due to electroporation.

3.2. Trapping and electrical response

Vesicles were trapped on the pore using pressures less than 0.7 N/cm^2. When trapped, the only current path in the device is through the seal between the vesicle and the pore in the nitride membrane. Therefore, upon trapping, the resistance increases by approximately a factor of 10, demonstrating that the membrane resistance is much larger than impedance contributions from the bulk solution and electrodes. When an applied voltage induced electroporation, a significant increase in the current was seen, resulting from an increase in vesicle membrane permeability. Fig. 4(A,B) are optical images of a giant vesicle before and after trapping.

A voltage waveform was generated that incremented from 0.5 to 2 V. The pulse duration and height of each incremental step were 100 ms and 0.1 V, respectively. As electroporation induced membrane permeability, a significant increase in the current was seen. We found the applied voltage needed to induce electroporation for five vesicles prepared using the first scheme was $V_A = 0.92 \pm 0.08$ V. The pressure used to immobilize vesicles from the first preparation method was $\Delta P = 0.36 \pm 0.23$ N/cm^2, and the vesicle diameters were $d = 18.0 \pm 4.9$ μm. Comparatively, the applied voltage needed for electroporation for five vesicles prepared using the second scheme was $V_A = 1.20 \pm 0.08$ V and the trapping pressure was $\Delta P = 0.27 \pm 0.06$ N/cm^2. All trapped vesicles were between 10–25 μm in diameter, with a mean and standard deviation of $d = 13.0$ μm and 0.90 μm, respectively. From these results, we found the applied voltage required to induce breakdown varied significantly between compositions. Fig. 5(A,B) illustrate typical electrical responses over time. The seal between the vesicle and the pore is not perfect; there is a small current path due to leakage around the vesicle, as shown in Fig. 3(B). By measuring the resistance due to this leakage, R_{LEAK}, at low voltages for each vesicle and assuming R_{LEAK} is constant, Fig. 5(A,B) show output current responses where an R_{LEAK} on the order of 3–4 MΩ is subtracted out. R_{LEAK} is a function of electrochemical effects and vesicle deformation during electroporation; however, we assume it is constant in the experimental data. For this reason, the fluorescence intensity was also monitored to visually verify electroporation. To clearly visualize the increase in current due to electroporation, Fig. 5(C, D) show output current versus input voltage corresponding to Fig. 5(A,B). Fig. 5(C,D) could also be used to calculate the variable resistances due to electroporation, R_{ELECT1} and R_{ELECT2} (illustrated in Fig. 3(B)), by fitting a line to the curve and taking the inverse of the slope of the line, m, where

$$R_{ELECT} = \frac{1}{m} = \frac{\Delta V}{\Delta I}. \quad (10)$$

We measured an R_{ELECT} of about 1 MΩ. Also, we estimate the membrane capacitance to be on the order of 1 pF, assuming a capacitance per unit area of 1 μF/cm^2 [25] suggesting a rapid charging time scale of 1 μs. We are interested in resolving changes in current during a 100 ms pulse, which are readily measured using our experimental setup, which has a resolution of approximately 70 μs. The time variations in the current in Fig. 5 are much slower than this, suggesting that the membrane itself is changing slowly under the applied load.

In addition to electrical evidence of electroporation, the fluorescence intensity was also measured to verify release of an analyte, such as a dye, during electroporation. Images were captured (two images per second), and the fluorescence intensity was subsequently measured by integrating the signal

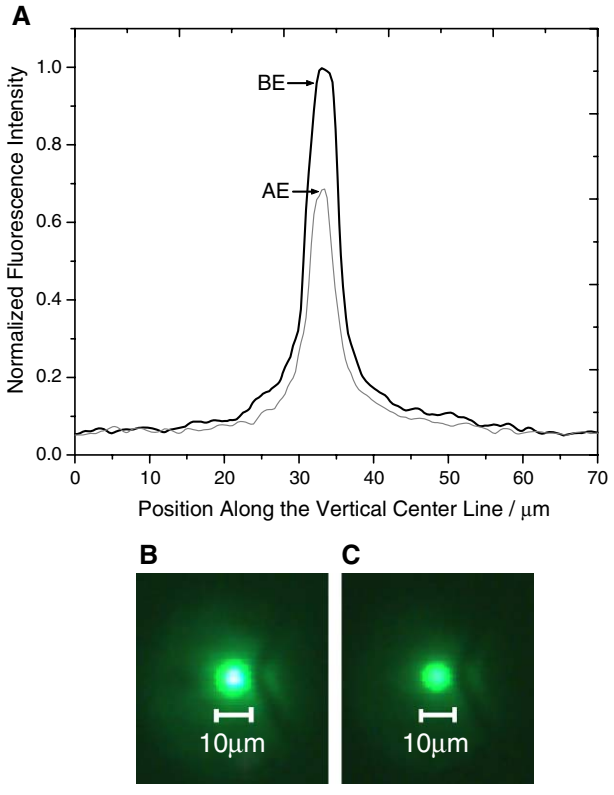

Fig. 7. (A) Light profile across vesicle before electroporation (BE) and light profile across vesicle after electroporation (AE). (B) Fluorescence image of a giant vesicle immobilized on the pore before electroporation, and (C) fluorescence image of the giant vesicle after electroporation, demonstrating dimming due to the release of dye from electroporation.

Table 1
Experimental data used in theoretical energy-based model presented in Section 2.6, where V_A is the external voltage applied, V_T is the transmembrane potential, ΔP is the applied pressure across the vesicle, d is the diameter of the vesicle, T_M is the mechanical energy stored per unit area of the vesicle membrane, T_E is the electrical energy stored per unit area of the vesicle membrane, and T is the total energy stored per unit area of the vesicle membrane

Composition		V_A (V)	V_T (V)	ΔP (N/cm^2)	d (μm)	T_M (mJ/m^2)	T_E (mJ/m^2)	T (mJ/m^2)
PEGDOPE : lecithin	Mean	0.92	0.86	0.36	18.0	8.4	1.8	10.2
	S.D.	0.08	0.06	0.23	4.9	5.2	0.27	5.0
PEGDSPE : lecithin	Mean	1.2	1.1	0.27	13.0	7.6	2.9	10.5
	S.D.	0.08	0.09	0.06	0.90	1.8	0.48	1.8

over the image (Fig. 6). In addition, the overall intensity in Fig. 7 was calculated by taking a light profile across the vesicle shown in Fig. 7 in the vertical direction. The increase in current during each pulse, the corresponding decrease in fluorescence intensity after each pulse (Fig. 6), and the overall intensity decrease (Fig. 7) demonstrate both electrical and optical evidence of electroporation. The vesicles did not release all of their dye after a given pulse, signifying that electroporation was reversible and the membrane eventually resealed after the application of the pulses. In general, while there may be a slight decrease in size as a result of electroporation, we found that there was no major change in the size and shape of the vesicle [26]. The intensity decrease is uniform over the entire vesicle, suggesting that it consists of a single compartment.

3.3. Comparison using theoretical model

Since the electrical and mechanical parameters (i.e., transmembrane potentials and applied pressures) varied for both vesicle compositions, the model of the stored energy in the membrane, presented in Section 2.6, was used to objectively compare the mechanical and electrical performance of the two vesicle compositions in our microfluidic device. The experimental data used in this model are summarized in Table 1. We found that there was no statistical difference in the energy required to induce electroporation between the two vesicle compositions. For the first composition, the energy to induce breakdown, T, was 10.2 ± 5.0 mJ/m^2. For the second composition, the mean energy to induce breakdown was 10.5 ± 1.8 mJ/m^2.

Interestingly, we found the electrical and mechanical energy contributions varied significantly for the two compositions. The critical electrical energy T_E, to induce breakdown was 1.8 ± 0.27 mJ/m^2 for the first vesicle composition, but 2.9 ± 0.48 mJ/m^2 for the second vesicle composition. These data lead us to believe that the vesicles made using the second preparation method are able to withstand more electrical stress than the vesicles made using the first method. In addition, we found the mechanical component, T_M, of the energy to induce breakdown was 8.4 ± 5.2 mJ/m^2 for the first vesicle composition, and 7.6 ± 1.8 mJ/m^2 for the second vesicle composition. This demonstrates that both vesicle compositions were statistically similar in the amount of mechanical stress they were able to withstand. It is difficult to discern at this stage whether these differences are due to chemical composition, vesicle size, or applied pressure. However, we found that our model provided consistent results, and both vesicle preparation methods presented here are suitable for manipulation in a microfluidic environment.

4. Conclusion

We have developed an improved preparation of giant vesicles that can be prepared easily and are robust enough to withstand simultaneous application of hydrostatic pressure and a strong electric field, as well as the relatively sharp edges frequently inherent to microfluidic designs. With these vesicles, we can controllably handle and electrically monitor picoliter volumes in a microfluidic environment. We have presented two versions of the preparation method and compared their performance in our prototype device platform. We have shown that these vesicles can be guided, trapped, and electroporated multiple times on a microfluidic electroporation chip, allowing for transfer of analytes, such as dye, from their confined environment.

The results in this study are the first steps towards a microfluidic sample management platform in which giant vesicles, robust enough to be utilized as picoliter reaction containers, are moved and manipulated by an electrical feedback control system between a number of sample loading stations, at which analytes are trapped in vesicles formed on the chip, combined with other encapsulated analytes, or released to initiate reaction, separation, or detection. While many tasks remain to integrate all of these functions and demonstrate reliability, we have shown that several of the key steps toward this new method to handle picoliter volumes in a microfluidic context are attainable through the electroporation of giant vesicles.

Acknowledgements

This work was performed by Sandia National Laboratories for the United States Department of Energy under contract DE-AC04-94AL85000. The authors acknowledge funding from Sandia Laboratory Directed Research and Development grants. The authors would also like to thank Ruben Diaz for fabrication of the chips, Bruce Mosier and Janson Wu for their assistance with the pressure measurements, and Carl Arft for his expertise in Matlab.

References

[1] T. Henkel, M. Bermig, M. Kielpinski, A. Grodrian, J. Metze, J.M. Kohler, Chip modules for generation and manipulation of fluid segments for micro serial flow processes, Chem. Eng. J. 101 (2004) 439–445.

[2] B.W. Ghidersa, A. Cacuci, Exploring the flow of immiscible fluids in a square vertical mini-channel by direct numerical simulation, Chem. Eng. J. 101 (2004) 285–294.
[3] J.C. Weaver, Y.A. Chizmadzhev, Theory of electroporation: a review, Bioelectrochem. Bioenerg. 41 (1996) 135–160.
[4] J. Weaver, Electroporation of biological membranes from multicellular to nano-scales, IEEE Trans. Dielectr. Electr. Insul. 10 (2003) 754–768.
[5] J.A. Lundqvist, F. Sahlin, M.A.I. Aberg, A. Stromberg, P.S. Eriksson, O. Orwar, Altering the biochemical state of individual cultured cells and organelles with ultramicroelectrodes, Proc. Natl. Acad. Sci. U. S. A. 95 (1998) 10356–10360.
[6] M. Khine, A. Lau, C. Ionescu-Zanetti, J. Seo, L. Lee, A single cell electroporation chip, Lab Chip 5 (2005) 38–43.
[7] Y. Huang, B. Rubinsky, Microfabricated electroporation chip for single cell membrane permeabilization, Sens. Actuators, A, Phys. A89 (2001) 242–249.
[8] R. Davalos, B. Rubinsky, Y. Huang, Electroporation: bio-electrochemical mass transfer at the Nano Scale, Microscale Thermophys. Eng. 4 (2000) 147–159.
[9] E. Neumann, A.E. Sowers, C.A. Jordan, Electroporation and Electrofusion in Cell Biology, Plenum Press, New York, NY, 1989.
[10] M. Karlsson, K. Nolkrantz, M.J. Davidson, A. Stromberg, F. Ryttsen, B. Akerman, O. Orwar, Electroinjection of colloid particles and biopolymers into single unilamellar liposomes and cells for bioanalytical applications, Anal. Chem. 72 (2000) 5857–5862.
[11] D.T. Chiu, C.F. Wilson, F. Ryttsen, A. Stromberg, C. Farre, A. Karlsson, S. Nordholm, A. Gaggar, B.P. Modi, A. Moscho, R.A. Garza-Lopez, O. Orwar, R.N. Zare, Chemical transformations in individual ultrasmall biomimetic containers, Science 283 (1999) 1892–1895.
[12] D. Needham, R.M. Hochmuth, Electro-mechanical permeabilization of lipid vesicles, Biophys. J. 55 (1989) 1001–1009.
[13] D.T. Chiu, C.F. Wilson, A. Karlsson, A. Danielson, A. Lundqvist, A. Stromberg, F. Ryttsen, M. Davidson, S. Nordholm, O. Orwar, R.N. Zare, Manipulating the biochemical nanoenvironment around single molecules contained within vesicles, Chem. Phys. 247 (1999) 133–139.
[14] K. Kuribayashi, S. Takeuchi, Formation of Monodisperse Giant Liposomes Using Micropatterned Lipid Films, 2005 Micro Total Analysis Systems (μTAS), October 9–13, 2005, Boston, Massachusetts, USA, 2005.
[15] M.I. Angelova, S. Soleau, P. Meleard, J.F. Faucon, P. Bothorel, Preparation of giant vesicles by external AC fields. Kinetics and application, Prog. Colloid & Polym. Sci. 89 (1992) 127–131.
[16] L.A. Bagatolli, E. Gratton, Two-photon fluorescence microscopy observation of shape changes at the phase transition in phospholipid giant unilaminar vesicles, Biophys. J. 77 (1999) 2090–2101.
[17] P. Bucher, A. Fischer, P.L. Luisi, T. Oberholzer, P. Walde, Giant vesicles as biochemical compartments: the use of microinjection techniques, Langmuir 14 (1998) 2712–2721.
[18] C. Schmidt, M. Mayer, H. Vogel, A chip-based biosensor for the functional analysis of single ion channels, Angew. Chem., Int. Ed. Engl. 29 (2000) 3137–3140.
[19] Y. Yamashita, O. Masato, T. Tanaka, M. Yamazaki, A new method for the preparation of giant liposomes in high salt concentrations and growth of protein microcrystals in them, Biochim. Biophys. Acta 1561 (2002) 129–134.
[20] G. Tresset, S. Takeuchi, Utilization of cell-sized lipid containers for nanostructure and macromolecule handling in microfabricated devices, Anal. Chem. 77 (2005) 2795–2801.
[21] R. Diaz, B. Rubinsky, A single cell study on the temperature effects of electroporation, 2004 ASME International Mechanical Engineering Congress and Exposition, November 13–20, 2004, Anaheim, California, USA, vol. 1, 2004.
[22] C.F. Wilson, G.J. Simpson, D.T. Chiu, A. Stromberg, O. Orwar, N. Rodriguez, R.N. Zare, Nanoengineered structures for holding and manipulating liposomes and cells, Anal. Chem. 73 (2001) 787–791.
[23] E. Evans, Minimum energy analysis of membrane deformation applied to pipet aspiration and surface adhesion of red blood cells, Biophys. J. 30 (1980) 265–284.
[24] H.P. Schwan, Electrical properties of tissue and cell suspension, Adv. Biol. Med. Phys. 5 (1957) 147–209.
[25] K.A. DeBruin, W. Krassowska, Modeling electroporation in a single cell. I. Effects of field strength and rest potential, Biophys. J. 77 (1999) 1213–1224.
[26] E. Tekle, R.D. Astumian, W.A. Friauf, P.B. Chock, Asymmetric pore distribution and loss of membrane lipid in electroporated DOPC vesicles, Biophys. J. 81 (2001) 960–968.